

THE PHYSICAL REVIEW

A Journal of Experimental and Theoretical Physics Established by E. L. Nichols in 1893

VOL. 50, No. 6

SEPTEMBER 15, 1936

SECOND SERIES

On the Allowed Cone of Cosmic Radiation

G. LEMAITRE AND M. S. VALLARTA, *University of Louvain and Massachusetts Institute of Technology*
(Received July 15, 1936)

Further results of an extensive study of trajectories asymptotic to a known family of unstable periodic orbits in the earth's dipolar magnetic field, carried out by means of Bush's differential analyzer, are presented in this paper. A detailed discussion is given of our methods of determining asymptotic trajectories by means of the differential analyzer and by numerical integration of a whole family at a time; comparison of the results obtained shows the absence of systematic errors of any consequence in the mechanical integrations and exhibits the precision attained with the differential analyzer. The families of asymptotic trajectories are then analyzed systematically in order to determine the main cones for latitudes up to 30° . This leads to the theory of the azimuthal effect and a study of the region in the vicinity of the zenith.

IN a preceding paper¹ to which reference should be made for a complete statement of the problem treated here and of our methods of attack, we gave results obtained from the analysis of some three hundred asymptotic trajectories to a known family of unstable periodic orbits found by means of Bush's differential analyzer² and discussed fully the sections of the main allowed cones of cosmic radiation by the meridian plane, which in turn led us to the theory of the north-south asymmetry. Those results were presented at the time with reservations as far as a critical examination of their precision was concerned. We have now been able to complete the calculations announced in our preceding paper, to which we shall return below, with the result that suspected systematic errors are so small that they can well be neglected. Certain other points which were then summarily sketched will now be developed in

detail; in particular we shall present here a full discussion of our method of determination of asymptotic trajectories by means of the differential analyzer and a fairly complete determination of the main allowed cones for geomagnetic latitudes up to 30° . The last two sections will be devoted to the analysis of the azimuthal effect and to a study of the region in the vicinity of the zenith.

1. THE DETERMINATION OF ASYMPTOTIC TRAJECTORIES BY MEANS OF BUSH'S DIFFERENTIAL ANALYZER

The differential equations of motion to be integrated are (reference 1, Eqs. (4), (5))

$$\begin{aligned}d^2x/d\sigma^2 &= (1/(2\gamma_1^4))e^{2x} - e^{-x} + e^{-2x} \cos^2 \lambda, \\d^2\lambda/d\sigma^2 &= e^{-2x} \sin \lambda \cos \lambda - (\sin \lambda / \cos^3 \lambda).\end{aligned}\tag{1}$$

Our problem is to find the solutions of these differential equations corresponding to trajectories asymptotic to a known family of unstable periodic orbits.

¹G. Lemaitre and M. S. Vallarta, *Phys. Rev.* **49**, 719 (1936).

²V. Bush, *J. Frank. Inst.* **212**, 447 (1931).

Before asymptotic trajectories can be studied, a full theory of the family of periodic orbits mentioned above must be available. The family in question was discovered by Störmer³ who was also able to calculate two of its members by his method of numerical integration. A complete treatment of the family has been given by one of us⁴ so that any one of its members can be calculated without great trouble and with high precision. While the details of these calculations would be out of place here and consequently are left for a separate paper, the results are reproduced in Fig. 1 where the small circles are the points on the periodic orbits of phase 0° , 15° , 30° , \dots , 90° which were computed. The equi-phase line 90° , i.e., the locus of the vertices of the periodic orbits which is important for our purpose as further discussed in a later section of this paper, has also been drawn in the figure.

Solutions of the system (1) representing the desired asymptotic trajectories and valid in the vicinity of the periodic orbits have been given by Bouckaert;⁵ other methods which we have recently developed and to which we return below are now available. In order to extend these solutions to the region of low energies and high latitudes, however, recourse must be had in general either to methods of numerical integration such as the one outlined in a later section of this paper or to methods of mechanical integration such as that developed by Bush,² because in general the system (1) cannot be integrated in terms of known functions. Since the knowledge of several hundred asymptotic trajectories is required for a satisfactory treatment of our problem the first line of attack involves a very large amount of tedious labor while the second can still be carried through in much shorter time.

An outline of our method of determination of asymptotic trajectories by means of Bush's differential analyzer has already been published.¹ Here we add only such details as are needed for a full understanding of our line of attack and of the results obtained. A first integration of the system (1) yields

³ C. Störmer, *Zeits. f. Astrophys.* **1**, 237 (1930).

⁴ G. Lemaître, *Ann. de la Soc. Sci. de Bruxelles* **A54**, 194 (1935).

⁵ L. Bouckaert, *Ann. de la Soc. Sci. de Bruxelles* **A54**, 174 (1935).

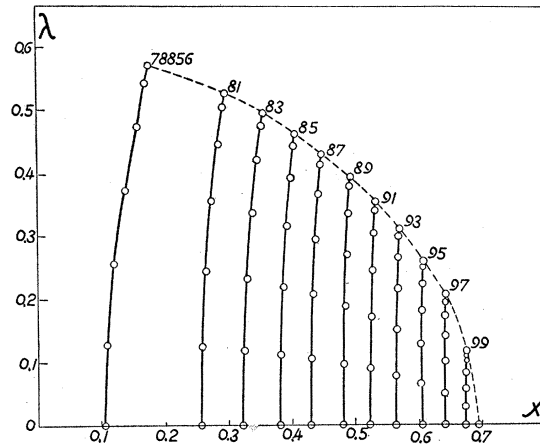


FIG. 1. The family of periodic orbits.

$$\begin{aligned} dx/d\sigma &= \int ((e^{4x}/16\gamma_1^4) - e^x + \cos^2 \lambda) e^{-2x} d\sigma, \\ d\lambda/d\sigma &= \int (e^{-2x} - (1/\cos^4 \lambda)) \sin \lambda \cos \lambda d\sigma. \end{aligned} \quad (2)$$

When written in the above form, suggested by S. H. Caldwell, the system (1) may be immediately set in the differential analyzer now available at the Massachusetts Institute of Technology and solved mechanically. This differential analyzer has ordinarily four input tables and six integrators, but an ingenious change in the machine connections devised for the present problem by S. H. Caldwell enables the use of the output table simultaneously as an input table so that in all five input tables and six integrators were available. Of these five input tables, two are needed to introduce in the machine the functions $e^{4x}/16\gamma_1^4 - e^x$ and e^{-2x} , and three more to introduce $\cos^2 \lambda$, $1/\cos^4 \lambda$ and $\sin \lambda \cos \lambda$. Of the six integrators, two are required to integrate the product of the two functions under the integral sign in each of the two equations (2), and two more to integrate the derivatives $dx/d\sigma$ and $d\lambda/d\sigma$ so as to obtain x and λ . The output table is then controlled so as to plot x as abscissa and λ as ordinate.

The scale factors are determined from the range of x and λ which it is desired to explore. For the present investigation the scales were so chosen that x could vary from -1.0 to 0.7 , λ from -0.7 to 1.0 , $dx/d\sigma$ and $d\lambda/d\sigma$ from -0.5 to 0.5 . The limits of the last two functions were found from a study of the energy integral (reference 1, Eq. (5)).

TABLE I. Data for some of the fundamental points.

$\gamma_1 =$ x	1 μ_0	0.87 η	0.90 η	0.93 η	0.96 η
0.075	3.1587	1.166	1.022	0.850	—
0.100	3.2127	—	—	—	—
0.125	3.2829	—	—	—	—
0.150	3.3670	1.211	1.062	0.890	—
0.175	3.4647	—	—	—	—
0.200	3.5790	—	—	—	0.721
0.225	3.7114	1.281	1.133	0.959	0.738
0.250	3.8608	—	—	—	—
0.275	4.0352	—	—	—	—
0.300	4.2342	1.371	1.266	1.051	0.821

TABLE II. Values of the initial angle for $\gamma_1=0.91$ for all equatorial runs.

x	ν	μ	η
0.075	-0.753	3.2265	0.968
0.100	-0.531	3.2605	0.978
0.125	-0.252	3.3056	0.992
0.150	0.084	3.359	1.008
0.175	0.380	3.431	1.029
0.200	0.760	3.511	1.053
0.225	1.276	3.596	1.079
0.250	1.914	3.689	1.107
0.275	2.745	3.788	1.136
0.300	3.650	3.907	1.172

The initial conditions are introduced into the machine knowing x , λ and the initial slope $\tan \eta$. The knowledge of x and λ is sufficient to set the starting points on the input tables. To set the starting points on each one of the six integrators it is necessary to calculate the values of the functions e^{-2x} ,

$$e^{4x}/16\gamma_1^4 - e^x + \cos^2 \lambda, \quad e^{-2x} - 1/\cos^4 \lambda, \\ \sin \lambda \cos \lambda, \quad dx/d\sigma \quad \text{and} \quad d\lambda/d\sigma.$$

The first four are computed from the known values of x and λ , the last two from the initial inclination η by the relations

$$dx/d\sigma = P^{\frac{1}{2}} \cos \eta; \quad d\lambda/d\sigma = P^{\frac{1}{2}} \sin \eta, \quad (3)$$

where P is given by Eq. (5).¹

For the efficient operation of the machine it is important that the calculations described above be carried out rapidly and accurately. For this purpose master sheets were prepared in advance giving the value of the required functions from $x = -0.125$ to $x = 0.350$ by intervals of 0.025 along the equator where P reduces to $e^{2x}/16\gamma_1^4 - (e^{-x} - 1)^2$ and for every degree of latitude along the line $\theta = 0$ where $P = e^{2x}/16\gamma_1^4$.

As already mentioned in our preceding paper,¹ for convenience trajectories were always started either from the equator or from the line $\theta = 0$. Once the master sheets are ready it is easy to calculate the initial conditions while the machine is tracing a trajectory, i.e., in the interval of a few minutes.

As already mentioned in our preceding paper one method for the determination of asymptotic trajectories consists in choosing a point on the equator within the periodic orbit and the initial slope arbitrarily. The initial conditions having been set on the machine, a trajectory is started in the direction towards the periodic orbit; the initial slope is then adjusted until the trajectory neither intersects nor falls short of the periodic orbit. More precisely let us suppose that the initial slope has been estimated not too far from the correct value, and assume for the sake of exemplification that the trajectory cuts through the periodic orbit. The initial angle is then increased by equal amounts, say of 0.008 radian until the trajectory falls decidedly short of the periodic orbit. The angle is then decreased by steps of 0.004 radian until the trajectory again cuts through, then increased by steps of 0.002 until the latter falls short, then again decreased by steps of 0.001 until it cuts through. In this way it is usually possible to determine the critical angle for an asymptotic orbit within around 0.001 radian by making from five to ten trials, each one taking from four to six minutes. That the critical angle is actually determined by this method with a precision of a few thousandths of a radian is confirmed by independent calculations of asymptotic trajectories to be more fully discussed in a later section of this paper.

In order to be free from the need of finding the critical angle for every equatorial point in the manner outlined in the preceding paragraph a method of interpolation was devised which permits the calculation of critical angles at intermediate points once the values at certain fundamental points have been ascertained. Let $\epsilon = 1 - \gamma_1$ and let

$$\mu_0 = \lim_{\gamma_1 \rightarrow 1} (\eta/\epsilon^{\frac{1}{2}}), \quad (4)$$

η being the initial critical angle for a given value of x . The quantity μ_0 may be calculated from

TABLE III. *Initial conditions for various values of γ_1 and values of $x < 0.075$ along the equator.*

γ_1 = x	0.87 η	0.89 η	0.91 η	0.93 η	0.95 η
-0.100	—	—	—	—	0.780
-0.075	—	—	—	0.890	0.747
-0.050	—	—	0.981	0.866	0.721
-0.025	—	—	0.965	0.852	0.707
0	1.160	1.050	0.957	0.840	0.703
0.025	1.155	1.050	0.956	0.840	0.705
0.050	1.163	1.055	0.960	0.842	0.711

Bouckaert's formulas⁵ for values of x greater than about 0.1 and is given in Table I above. Let now μ be the corresponding quantity for $\gamma_1 \neq 1$. We have

$$\mu = \eta / \epsilon^{\frac{1}{2}}, \quad (5)$$

where η is now determined by the trajectories traced by the differential analyzer as outlined above. Let us place

$$\mu = \mu_0 - \nu \epsilon. \quad (6)$$

Our process of interpolation consists in finding η for certain fundamental points and then calculating ν from it by the use of the formulas written above; ν is then plotted to an appropriate scale as a function of γ_1 for each chosen value of x through which we desire to have an asymptotic trajectory. For interpolated points ν is determined from these plots knowing x and γ_1 , μ is then calculated and finally η . Table I gives the data for some of the fundamental points.

As an example of the use of the method of interpolation we give in Table II the values of the initial angle for $\gamma_1 = 0.91$ for all equatorial runs.

Similar tables were prepared for all other values of γ_1 which were studied (reference 1, p. 722). In all over one hundred asymptotic trajectories starting from equatorial points were thus determined. In order to verify interpolated values a few trajectories were continued as far as the periodic orbit with very satisfactory results. That the precision of interpolated trajectories is as high as that of trajectories through fundamental points will be shown in the next section.

For points on the equator for which μ_0 cannot be calculated from Bouckaert's formulas, i.e., for very small and for negative values of x , the initial angle was determined from the condition

that an asymptotic trajectory must be tangent to the envelope of the asymptotic family which was known from those asymptotic trajectories already found. As a further verification the trajectories were continued in some cases as far as the periodic orbit, but because of the sharpness of the turns when such asymptotic orbits oscillate in the vicinity of the periodic orbit the ordinary condition for an asymptotic trajectory cannot be ascertained with precision by means of the differential analyzer. As an example we give in Table III the initial conditions for a few of the values of γ_1 we have studied and values of $x < 0.075$ along the equator.

As regards asymptotic trajectories starting from the line $\theta = 0$ the procedure was similar to that described above: the criterion determining an asymptotic trajectory was that it must be tangent to the envelope of the asymptotic family. The interpolation was made directly on the initial angle, the procedure being to plot to an appropriate scale η as a function of λ for each value of γ_1 from a few fundamental points and then to read off from the plot the value of η for intermediate values of λ . Curves showing the relation between the critical angle and the latitude for all values of γ_1 along the line $\theta = 0$ have already been published (Fig. 5, reference 1). As an example the values of the critical angle for fundamental points corresponding to $\gamma_1 = 0.85$ are given in Table IV:

Examples of families of asymptotic trajectories are given in Fig. 2. In this figure portions of trajectories intercepted by the earth are shown dotted, i.e., for these portions a parallel to the λ -axis cuts a preceding part of the trajectory.

TABLE IV. *Values of the critical angle for fundamental points for $\gamma_1 = 0.85$.*

λ (deg.)	η	η_1
-23	2.170	—
-20	—	2.326
0	1.253	1.885
5	1.140	—
10	1.035	—
15	0.915	1.451
20	0.794	1.235
25	0.603	0.975
26	0.562	0.915
27	0.523	0.830
28	0.515	0.750
29	—	0.600

A few trajectories of the third kind and a self-reversing doubly asymptotic trajectory with self-reversal point T_2 (cf. reference 1, sec. 4, Fig. 4) are clearly seen.

2. PRECISION OF ASYMPTOTIC TRAJECTORIES

In this section we present an outline of a method of calculation of asymptotic trajectories which we have developed recently in order to investigate systematic errors in the trajectories found by means of the differential analyzer. The details are reserved for a paper to appear shortly in the *Annales de la Société Scientifique de Bruxelles*. It will be seen that systematic errors in asymptotic trajectories determined by means of the differential analyzer are small enough that they can well be neglected, except for very high latitudes, and that the precision attained throughout is very satisfactory.

The family of asymptotic trajectories is represented by a trigonometrical series in $\omega\sigma + \varphi$, where $2\pi/\omega$ is the period and φ the arbitrary phase of the periodic orbit. We have

$$x = \sum_k [y_k(\sigma) \sin k(\omega\sigma + \varphi) + z_k(\sigma) \cos k(\omega\sigma + \varphi)] \quad (7)$$

and a similar expression for λ with amplitudes μ, ν in which k takes even integral values in the expansion for x and odd values in that for λ . The asymptotic behavior of $y(\sigma)$ and $z(\sigma)$ is exhibited by the expression for z_k :

$$z_k(\sigma) = z_k + z_k' e^{\Omega\sigma} + z_k'' e^{2\Omega\sigma} + \dots, \quad (8)$$

where z_k, z_k', z_k'' are numerical coefficients of which the first corresponds to the periodic orbit. The variational equation then yields a set of linear and homogeneous equations the determinant of which must vanish. This condition, i.e., the "secular equation," determines the real characteristic exponent Ω . We have thus computed the first and second order terms in $e^{\Omega\sigma}$. The second order term of z_0 is rather large, so that a more convenient approximation had to be derived. This approximation is suggested by previous investigations of one of us and of Bouckaert⁵ for the case where γ_1 differs slightly from 1. Writing

$$e^{-z_0(\sigma)} = e^{-z_0}(1+u), \quad (9)$$

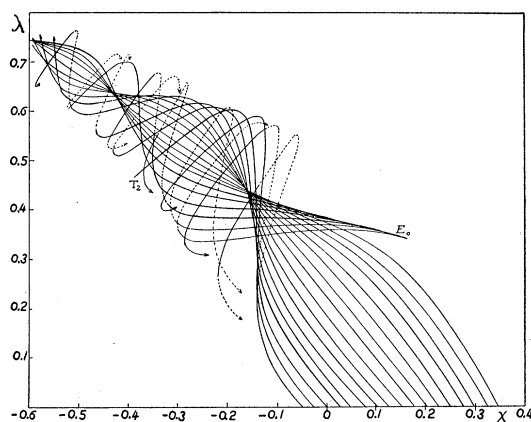


FIG. 2. A family of asymptotic trajectories. $\gamma_1=0.93$.

we have taken as approximation a solution of the equation

$$(du/\Omega d\sigma)^2 = u^2(1+bu+cu^2), \quad (10)$$

where the constants b and c are determined more or less empirically. By this means it was found possible to use the expansion up to a distance 0.048 from the periodic orbit. Careful numerical checks proved it to be correct to the sixth decimal. Difference tables of the functions $y(\sigma)$, $z(\sigma)$ and the corresponding functions $\mu(\sigma)$, $\nu(\sigma)$ in the expansion for λ were then prepared for the six preceding values of σ with an interval corresponding to $\omega\Delta\sigma=15^\circ$, i.e., $\Delta\sigma=0.293243$. While the functions y, z , etc., vary very slowly the corresponding trajectories perform many very close oscillations in the vicinity of the periodic orbit so that their calculation by the usual methods of numerical integration would be extremely difficult, in any case requiring a much smaller interval $\Delta\sigma$. For this reason instead of integrating numerically the differential equations of motion in order to find the trajectories we have preferred to integrate the differential equations of the amplitudes y, z , etc.

The differential equations satisfied by these functions can be found as follows: replacing x and λ by their series expressions and expanding in a trigonometrical series we may write

$$\frac{1}{2}\partial P/\partial x = \sum_k [Y_k(\sigma) \sin k(\omega\sigma + \varphi) + Z_k(\sigma) \cos k(\omega\sigma + \varphi)]. \quad (11)$$

This defines Y and Z as a function of y, z, μ

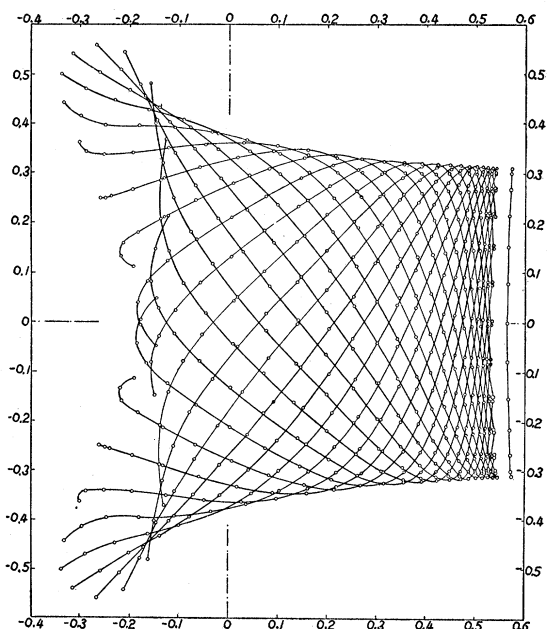


FIG. 3. Calculated family of asymptotic trajectories. $\gamma_1=0.929898$.

and ν because of the equations of motion (1). For practical use of this equation we may take advantage of the fact that with the exception of z_0, μ_1 and ν_1 all the other terms are small and powers higher than the second may be neglected. In any case ν_1 can be made to vanish by a suitable change of the phase angle. Once the phase has been shifted explicit expansion can be derived with coefficients depending on z_0 and the new μ_1' , and included in a convenient computation schedule. Finally the phase must be shifted back to its original value.

The equations to be integrated are of the form

$$\begin{aligned} (d^2y_k/d\sigma^2) - 2k\omega(dz_k/d\sigma) - k\omega^2y_k &= Y_k, \\ (d^2z_k/d\sigma^2) + 2k\omega(dy_k/d\sigma) - k\omega^2z_k &= Z_k, \end{aligned} \tag{12}$$

and similar equations for μ_k and ν_k . Ordinary methods of integration such as Adams' would have been impracticable as they would be tantamount to an attempt to calculate a sine from its second order differential equation using intervals of $15^\circ, 30^\circ, \dots, 90^\circ$ according to the value of k . Introducing the complex notation $x=y+iz, X=Y+iZ$ and taking the case $k=1$ as typical, the above equations may be written

$$(d^2/d\sigma^2)(xe^{i\omega\sigma}) = Xe^{i\omega\sigma}, \tag{13}$$

which yields upon integration and elimination of integration constants by taking second differences

$$\Delta^2xe^{i\omega\sigma} = \Delta^2 \iint X e^{i\omega\sigma} d\sigma^2. \tag{14}$$

When $\omega=0$ we fall back on Störmer's method of numerical integration. The question now is to devise a suitable method of integration for the present equation.

$$\text{Writing } \omega\sigma = w(t_0+t), \tag{15}$$

where t is the ordinal number of the integration points and w is the interval of integration, and supposing that the values of x_n, X_n are known up to $n=-1$, the question is to compute the value of x_0 as a function of $x_{-1}, x_{-2}, X_{-1}, \delta X_{-1} = X_{-1} - x_{-2}, \delta^2x_{-1} = \delta x_{-1} - \delta x_{-2}$, etc. The left-hand member of the equation

$$\Delta^2xe^{\alpha t} = w^2 \iint X e^{\alpha t} dt, \tag{16}$$

where $\alpha = i\omega w$ is $x_0 - 2e^{-\alpha}x_{-1} + e^{-2\alpha}x_{-2}$. X may be expressed as a function of X_{-1} and its successive differences by

$$X(t) = \sum_k (1/k!)(t+1)(t+2)\dots(t+k)\delta^k X_0. \tag{17}$$

If $D = \partial/\partial\alpha$ we have

$$\iint t^n e^{\alpha t} dt^2 = D^n \iint e^{\alpha t} dt^2 = D^n (e^{\alpha t}/\alpha^2) \tag{18}$$

and the final relation is

$$\begin{aligned} x_0 &= 2e^{-\alpha}x_{-1} - e^{-2\alpha}x_{-2} + \sum_k w^2 (1/k!)(D+1)(D+2) \\ &\quad \dots (D+k)(1 - 2e^{-\alpha} + e^{-2\alpha}/\alpha^2)\delta^k X_{-1} \\ &= 2e^{-\alpha}x_{-1} - e^{-2\alpha}x_{-2} + \sum_k a_k \delta^k X_{-1}. \end{aligned} \tag{19}$$

Returning to real variables and writing $a_k = b_k + ic_k$ we have finally the working formulas

$$\begin{aligned} y_0 &= 2 \cos \omega w \cdot y_{-1} - y_{-2} \cos 2\omega w \\ &\quad + 2z_{-1} \sin \omega w - z_{-2} \sin 2\omega w \\ &\quad + w^2 (\sum_{k=0} b_k \delta^k Y_{-1} - \sum_{k=0} c_k \delta^k Z_{-1}) \end{aligned} \tag{20}$$

and

$$\begin{aligned} z_0 &= 2z_{-1} \cos \omega w - z_{-2} \cos 2\omega w \\ &\quad - 2y_{-1} \sin \omega w + y_{-2} \sin 2\omega w \\ &\quad + w^2 (\sum_{k=0} b_k \delta^k Z_{-1} + \sum_{k=0} c_k \delta^k + Y_{-1}). \end{aligned} \tag{21}$$

The coefficients b_k, c_k have been computed up to $k=4$, i.e., up to and including the fourth difference and for $\omega\Delta\sigma = 15^\circ, 30^\circ, \dots 90^\circ$ corresponding up to the sixth harmonic.

The integration has been actually carried out for twenty steps until the region was finally reached where the change of the integrated functions became so large that the integration could no longer be continued without splitting the interval of integration. The family of twenty-four trajectories, symmetrical in pairs, has been computed and is shown in Fig. 3. For a table of the computed points reference must be made to the complete paper. The small circles shown in the figure are calculated points for which the phase is $0^\circ, 15^\circ, \dots 90^\circ$ and correspond with those shown on the periodic orbits (Fig. 1).

The comparison with the asymptotic trajectories found by means of the differential analyzer is shown in Fig. 4. It is seen that the agreement is excellent particularly as regards the position of the cusp C_0 . One of the machine trajectories starting from $x=0.275$ and $\lambda=0^\circ$ happens to have a value of φ_0 equal to that of the calculated trajectory and both coincide, the others have different values of φ_0 but that they all belong to the same family can be tested by analyzing their general shape and proved by the fact that they all are tangent to the same envelope. As a matter of fact the consistency between calculated and machine trajectories is as good as that found among the machine trajectories themselves. A more precise comparison may be made by calculating the value of the inclination η of three fundamental trajectories at the equator. The result is shown in Table V.

3. DETERMINATION OF THE ALLOWED MAIN CONE

The theory of the main cone, or region of full light, has already been outlined in our previous papers. A sketch of our method for its determination and its representation, once the families

TABLE V. Calculated values of the inclination η of three fundamental trajectories at the equator.

x	η (mach.)	η (calc.)	Diff.
0.150	0.890	0.887	0.003
0.225	0.959	0.953	0.006
0.300	1.053	1.045	0.008

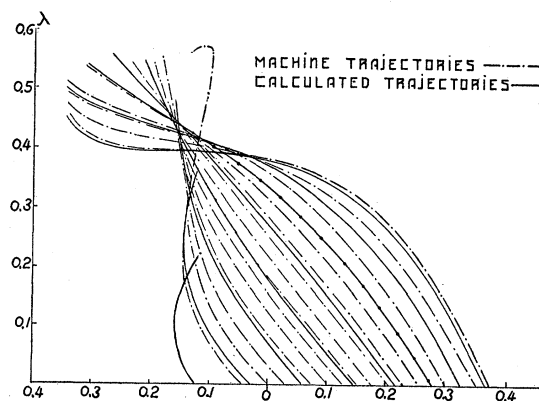


FIG. 4. Calculated asymptotic trajectories compared with trajectories obtained with differential analyzer. $\gamma_1 = 0.93$.

of asymptotic trajectories have been found, has also been given in our preceding paper (reference 1, p. 724). The coordinates of a representative point are $\sin \theta$ and $\cos \theta \sin \eta$; for positive particles θ and η are counted positively eastwards and northwards, respectively. Let us assume an asymptotic trajectory passing through a point of coordinates x and λ ; η is then the angle with the zenith direction, i.e., with a parallel to the x axis and θ the angle between the trajectory and the meridian plane which can be immediately calculated from Störmer's formula (reference 1, Eq. (1)). The energy r in Störmer's corresponding to the given x is then given by Eq. (2).¹ We thus obtain a point of the representation of the cone for the given values of the energy and the latitude.

For the systematic utilization of the asymptotic trajectories traced by the differential analyzer two lines of attack are open. Either one may first calculate from Störmer's formula the lines $\theta = \text{const.}$ for all values of γ_1 for which asymptotic trajectories were studied and then measure the values of the angle η along these lines noting at the same time the value of x . This is equivalent to determining sections of the cones of different energies and at different latitudes by planes parallel to the meridian plane. Suppose that the lines $\theta = 0^\circ, 5^\circ, 10^\circ, \dots$ have been computed for $\gamma_1 = 1.00, 0.99, 0.98, \dots 0.78$, and the angles η measured along each. Then plots may be readily constructed giving the angle η as a function λ for each value of γ_1 and, besides, the energy r as a function of x for each

value of γ_1 . This is the method used for $\theta=0^\circ$ in our preceding paper¹ where diagrams giving η as a function of λ for each value of γ_1 are given (Fig. 5, reference 1). It has not been used for other values of θ because the computation of the lines $\theta=\text{const.}$ is laborious. Once these have been found, however, the calculation of the cone is immediate.

An alternative line of attack is to measure the inclination η along the lines $\lambda=\text{const.}$ for each value of γ_1 which was studied, noting at the same time the value of x where the intersection between the asymptotic trajectory and the chosen line $\lambda=\text{const.}$ takes place. Graphs may then be drawn showing η as a function of r for each chosen value of λ , for example $\lambda=0^\circ, 5^\circ, 10^\circ \dots$ and different values of γ_1 .⁶ An envelope is characterized on these ηr -diagrams by a point of tangency of η as a function of r with a line parallel to the η -axis, i.e., by a turning point for a maximum or minimum value of r . A cusp is characterized by the coalescence of two such points; it is a point of inflection with a tangent parallel to the η -axis. These peculiarities of the ηr -diagrams are reflected in the representation of the cone; their significance has already been taken up fully in our preceding paper.¹ If on the ηr -diagrams a value $r=\text{const.}$ is picked out it is readily seen that the boundary of the cone progresses eastwards (for positive particles) as γ_1 increases.

The main cones for $\lambda=0^\circ, 20^\circ$ and 30° are reproduced in Figs. 5, 6 and 7. The small circles are the points calculated by Bouckaert.⁵ It is seen that except for high zenith angles and low energies the agreement is again quite satisfactory. The extreme northern part of the main cone where the shadow of the earth makes itself felt is given with reservations as a detailed analysis of the trajectories of the second and third kinds outside of the meridian plane still remains to be made.

4. THE AZIMUTHAL EFFECT

We begin by recalling that in addition to the main cones determined as described in the

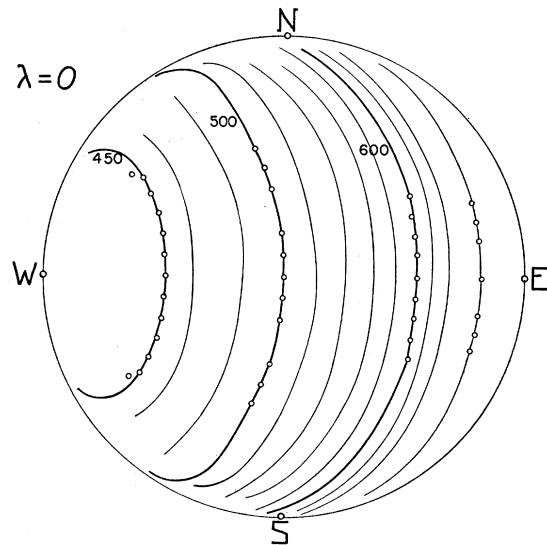


FIG. 5. The main cones. Energies in millistörmers. Positive particles, northern hemisphere.

previous paragraph there is also the region of penumbra. While the full analysis of the latter must be left to another occasion preliminary results obtained with the differential analyzer and earlier by one of us⁷ show that there are bands of light of complicated structure running alongside the boundary of the main cone alternating with bands of darkness and extending eastwards (for positive particles) clear over to Störmer's limiting cone⁸ of total darkness at the value of θ corresponding to the given latitude and energy and to $\gamma_1=1$. While the chief contribution to the azimuthal effect as described later in this paragraph undoubtedly comes from the main cones the theory here presented must be improved later, particularly as regards the east-west asymmetry, so as to take the penumbra into account. Another correction must also be made to take care of the eccentricity of the earth's magnetic center. This correction at a given point on the earth affects only the energy scale and can readily be computed by methods already given in a previous paper.⁹

A consideration of the main cones drawn in Figs. 5 to 7 shows immediately that the range of

⁶ This laborious piece of work was carried out by Mr. L. de Borman and forms part of his master's thesis at the University of Louvain, 1936, from which Figs. 5, 6 and 7 are taken.

⁷ G. Lemaitre, *Ann. de la Soc. Sci. de Bruxelles* **A54**, 162 (1935).

⁸ C. Störmer, University Observatory, Oslo, Publication No. 10 (1934).

⁹ M. S. Vallarta, *Phys. Rev.* **47**, 647 (1935).

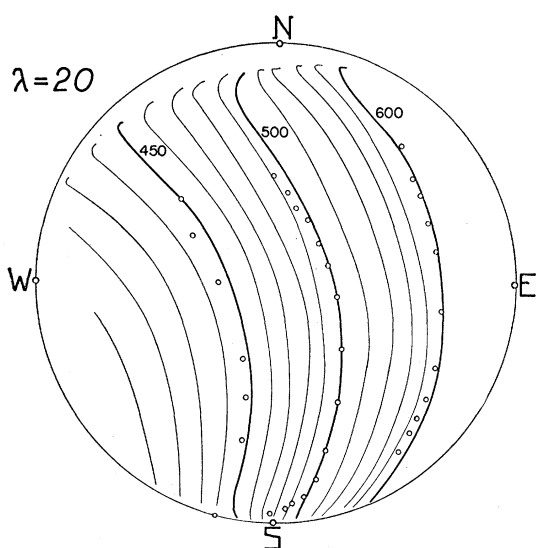


FIG. 6. The main cones. Energy in millistörmers. Positive particles, northern hemisphere.

energy which can reach a point on the earth at a given zenith angle z is not the same at all azimuths. Consequently there must be a variation of intensity at a fixed zenith angle and different azimuths (azimuthal effect). Special cases of the azimuthal effect are the north-south and east-west asymmetries. Suppose now that the circles $z = \text{const.}$ are drawn on the diagrams representing the cones (Figs. 5 to 7). These intersect the boundaries of the cones of different energies at azimuths which can be read off directly on the figures. In this way the curves, Fig. 8, are obtained which give the minimum energy capable of reaching a given latitude at a zenith angle of 45° and azimuths shown by the curves. Similar curves for other zenith angles may be readily found.

Unfortunately no systematic comparison with the experimental azimuthal effect is possible at the present time because no systematic measurements covering the complete turn of the horizon have been made. The most complete data available are those of Johnson¹⁰ who has made measurements at different azimuths and fixed zenith angles with a triple coincidence counter system covering more or less thoroughly the horizon from east to west through south. These measurements were made in Mexico ($\lambda = 29^\circ$),

¹⁰ T. H. Johnson, *Phys. Rev.* **45**, 569 (1934).

Panama ($\lambda = 20^\circ$) and Peru ($\lambda = 0^\circ$) at zenith angles 45° and 30° and heights of 6.8 m, 10 m and both 6.8 m and 6 m, respectively below the top of the equivalent water atmosphere. While no significant quantitative conclusions seem warranted at the present time there is good qualitative agreement between theory and experiment even without resorting to negative primaries. An important point brought out by the Peruvian experiment is that the addition of an atmospheric depth equivalent to 0.8 m of water does not change the relative order of the intensities with respect to one another. This must be expected if the azimuthal effect is essentially due to the action of the earth's magnetic field on the primaries because, since the zenith angle is constant, the length of the atmospheric path traversed by the rays is the same at all azimuths.

Besides the north-south asymmetry, already discussed extensively in our preceding paper,¹ an interesting case of the azimuthal effect is the east-west asymmetry first discussed by Rossi.¹¹ Historically this was the first case of the azimuthal effect to be discovered and has since been thoroughly studied experimentally; perhaps we may be permitted here to voice the regret

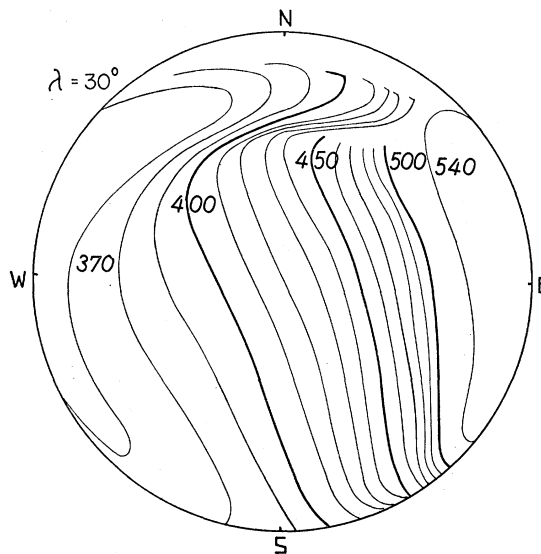
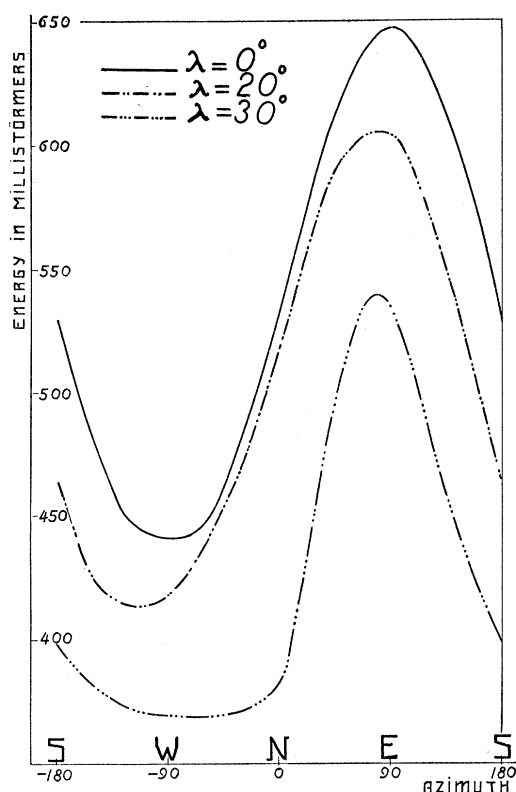


FIG. 7. The main cones. Energy in millistörmers. Positive particles, northern hemisphere.

¹¹ B. Rossi, *Phys. Rev.* **36**, 606 (1930), see also *Ricerca Scientifica* **1**, 561 (1934) for full references to his previous work.

FIG. 8. The azimuthal effect for $z=45^\circ$.

that it has been studied practically to the exclusion of all other azimuths. Fig. 9 shows a comparison of the energy ranges involved in the east-west and north-south asymmetries, where the former refers to positive particles and the latter to particles of either sign. It is immediately apparent that for purposes of gaining information as to the energy distribution of the primary radiation the study of the north-south asymmetry is superior to that of the east-west, first because the penumbra acts mainly on the east-west asymmetry but hardly on the north-south, second because the energy range is smaller and third because the north-south is independent of the particles' sign. Except that the interpretation of the east-west asymmetry is made difficult because of the penumbra, a comparison between the east-west and north-south asymmetries furnishes a means, already pointed out in a previous paper, of determining the percentage of particles of either sign. A consideration of the curves in Fig. 9 shows that if the primary cosmic radiation is made up entirely of particles of one sign the

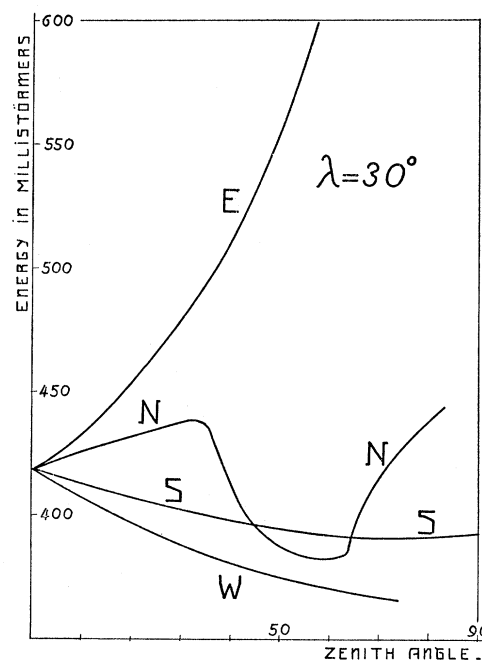


FIG. 9. The east-west and north-south asymmetries. Positive particles, northern hemisphere.

north-south asymmetry must be considerably smaller than the east-west. A mixture of positive and negatives on the other hand, decreases the east-west asymmetry but leaves the north-south unaffected, provided the energy ranges covered by positives and negatives are not the same. Thus Johnson's measurements in Mexico of the north-south and east-west asymmetries would seem to leave room for positive and negative primaries.¹²

It should also be noted that once the cones have been calculated it is quite feasible to take the finite aperture of a multiple coincidence counter system into account. Failure to consider this point may easily lead into error when interpreting experimental results.

5. THE MAIN CONE IN THE VICINITY OF THE ZENITH

A particularly interesting region from the point of view of intensity measurements is the region around the zenith to which Zanstra¹³ has already called attention. We intend to devote this section to the study of this region.

¹² T. H. Johnson, Phys. Rev. **47**, 91 (1935); **48**, 290 (1935).

¹³ H. Zanstra, Naturwiss. **22**, 171 (1934).

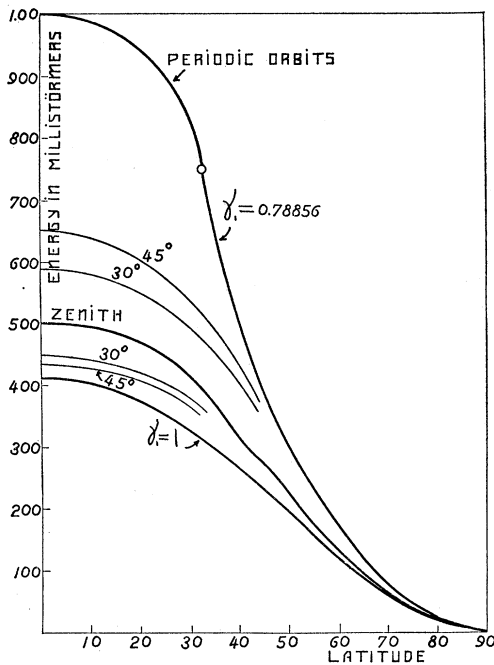


FIG. 10. Minimum energies in the region near the zenith.

In the vicinity of the zenith the boundaries of the main cones run almost parallel to one another and intersect the meridian plane at a small angle ψ which increases with latitude. The value of the energy r for which the boundary of the main cone goes through the zenith gives the minimum energy that a particle must have to reach the earth in the vertical direction at a given latitude. This can be readily found by interpolation from the data contained in Figs. 5 to 7 or from the equation of the line $\theta=0$

$$e^x = 2\gamma_1 r = \cos^2 \lambda, \quad (22)$$

where the dependence of γ_1 on longitude in the zenith direction is given by Fig. 5 of our preceding paper.¹ This minimum energy is given in Fig. 10 together with other curves the significance of which will be taken up later. The angle ψ is plotted as a function of latitude in Fig. 11 together with the gradient dr/dz at the zenith. It is seen that the gradient varies slowly with the latitude, nevertheless it is of importance when interpreting vertical intensity measurements made with triple coincidence counter systems of large aperture. The orientation of the counter system with respect to the direction ψ is also a significant datum of the experiment.

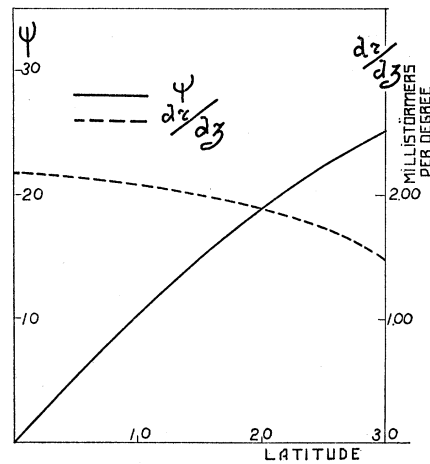


FIG. 11. The angle between the main cone and the meridian plane and the energy gradient at the zenith.

The importance of the knowledge of the least vertical energy, emphasized by Zanstra, arises from the fact that, if the spectrum of the cosmic radiation is a continuous function of the energy, then intensity measurements in the vertical direction made beginning at the equator and extending sufficiently far north or south give a ready means of estimating with fair accuracy the energy lost by a cosmic-ray particle while traversing the atmosphere. It is sufficient to find the latitude beyond which the vertical intensity remains constant. Unfortunately neither the vertical intensity measurements of Auger and Leprince-Ringuet¹⁴ nor those of Clay¹⁵ between $\lambda=10^\circ$ and $\lambda=20^\circ$ under 20 cm of lead extend sufficiently far north or south to make this estimate possible.

Another interesting question which can now be answered is as to the energy range which can reach a point of the earth of latitude λ coming from directions at a zenith angle z . For latitudes up to 30° the energy range involved can be read off directly from Figs. 5 to 7. The corresponding curves are plotted in Fig. 10. Their significance will be clear from the following example. Suppose we take $\lambda=30^\circ$ and ask what is the energy range which may arrive within the cone bounded by the directions at 45° with the zenith. The lower curve for $z=45^\circ$ then shows that 362 millistörmers is the minimum energy that a particle

¹⁴ P. Auger and L. Leprince-Ringuet, *Nature* **133**, 138 (1934).

¹⁵ J. Clay, *Physica* **2**, 308 (1935).

must have to arrive at 45° from the zenith (and in a certain azimuth) while the upper curve gives that if it has a minimum energy of 540 millistörmers it may arrive from any direction within 45° of the zenith. Similarly 408 millistörmers is the least energy a particle must have to arrive at 30° from the zenith, while 510 millistörmers is the least energy required to arrive from any direction within 30° of the zenith. In addition the limiting energies for which the main cone is completely open is given by the uppermost curve. This curve consists of two parts: first, the locus of the vertices of the periodic orbits (cf. Fig. 1) and then the limiting energy for the limit $\gamma_1 = 0.78856$ for which periodic orbits disappear. This curve takes into account only the trajectories of the

first kind.¹⁶ Finally the lowest curve gives the limiting energy for Störmer's limit $\gamma_1 = 1$ for which all directions are forbidden.

It is a pleasure to renew the expression of our gratitude to the various persons, mentioned in our preceding paper, who have helped us to carry out the research of which this paper is another fruit. One of us is indebted to the Massachusetts Institute of Technology for continued support while this investigation was being completed at Louvain, and to the University of Louvain for providing numerous facilities during the period of his residence there.

¹⁶ For trajectories of the second kind a somewhat higher energy limit can be readily found from the relation $e^{\frac{x}{\lambda}} \leq 2 \cos \lambda$ above which the acceleration $d^2x/d\sigma^2$ is necessarily positive. For the same reason negative values of γ_1 are of no interest.

Excitation-Curves for Fluorine and Lithium

L. R. HAFSTAD, N. P. HEYDENBURG AND M. A. TUVE, *Department of Terrestrial Magnetism, Carnegie Institution of Washington*

(Received July 6, 1936)

Observations on the alpha-particles emitted by lithium and the gamma-rays emitted by lithium and fluorine when bombarded with protons of energies up to 1000 kv have been improved by the use of a corona-free, 10,000-megohm voltmeter-resistor for voltage-measurements. By this means the accuracy of our measurements has been brought to two percent on an absolute scale and about one percent on a relative scale. Oscillograph-studies of voltage-fluctuations have shown that up to 1000 kv the voltage is constant to ± 1.4 percent "peak-ripple." For the distribution-curve for voltage *versus* time the "half-maximum" width is about one percent at 1000 kv. Results thus far obtained for the

gamma-ray resonances are as follows:

Voltage	Element	Half-width
328 kv	F	< 4 kv
440 kv	Li	11 kv
892 kv	F	< 12 kv
942 kv	F	< 15 kv

There is an indication of a weak multiplet structure in fluorine in the region between 500 and 700 kv with a broad but fairly prominent "resonance" at 650 to 700 kv. The existence of a resonance in lithium at 850 kv was not confirmed.

INTRODUCTION

OUR work on proton-disintegrations last year¹ demonstrated the existence of sharp resonance-effects in nuclear disintegrations which called for voltage-control considerably more refined than that given by any apparatus then in existence. Such work depends essentially on the accurate reproducibility of specified voltages, and this requirement is not sufficiently well

¹Hafstad and Tuve, *Phys. Rev.* **48**, 306 (1935); also Tuve, Hafstad and Dahl, *Phys. Rev.* **48**, 315 (1935).

satisfied even by rectifier and condenser installations, unless means for voltage-measurements more accurate than spark-gap or particle-range determinations are provided. Unless very special precautions are taken, sphere-gap measurements are rarely reproducible to better than five percent. Even the official calibration-curves for sphere-gaps have been changed by more than ten percent during the past two years. The absence of reliable information on the range-energy relation for protons would prevent the